Journal of
Applied
Crystallography
ISSN 0021-8898

Received 23 July 1999
Accepted 4 November 1999

On the instrumental resolution in X-ray reflectivity experiments

D. Sentenac, A. N. Shalaginov, A. Fera and W. H. de Jeu*

FOM Institute for Atomic and Molecular Physics, Kruislaan 407, 1098 SJ Amsterdam, The Netherlands. Correspondence e-mail: dejeu@amolf.nl

A general method to describe the instrumental resolution function for grazing-angle X-ray scattering experiments is presented. A resolution function $\mathcal{R}$ is introduced as the Gaussian joint-distribution function of the (interdependent) random deviation $\mathbf{q}'$ associated with the wavevector transfer $\mathbf{q}$. Useful expressions for the mean square values of $\mathbf{q}'$ are derived for some common scattering geometries, such as rocking scans, and scans out of the plane of incidence. The mean square values related to the incident beam dispersion and the detector acceptance angles are included in the treatment of $\mathcal{R}$. As an example, $\mathcal{R}$ is incorporated in the calculation of the diffuse scattering from free-standing smectic films within the framework of the first Born approximation and the main resolution effects are discussed.

1. Introduction

Grazing-angle X-ray scattering is being extensively used to study the structure and interfacial properties of hard and soft thin films. As an example, X-ray reflectivity and surface diffraction are powerful techniques to probe normal and in-plane structures on the molecular scale (*e.g.* Holý *et al.*, 1999), and X-ray diffuse scattering has been shown to be very useful in determining the interfacial properties of thin liquid films, such as the surface tension and bending elasticity modulus (*e.g.* Gompper & Schick, 1994; Tolan, 1999). In all these experiments, the experimental resolution must be carefully taken into account as the physical information is intimately mixed up with it. The origin of the resolution stems from the properties of the particular scattering geometry pictured in Fig. 1 for a z-axis setup. The vector $\mathbf{k}_{\rm in}$ defines the direction of the beam incident on the sample; the plane defined by the (Oz) axis and $\mathbf{k}_{\rm in}$ is called the plane of incidence. The direction of $\mathbf{k}_{\rm in}$ is experimentally defined by α_i and α_o. The incident beam has in general a rectangular cross section defined by two orthogonal sets of slits S_{E_i} and S_{E_o} perpendicular to $\mathbf{k}_{\rm in}$ (pre-sample slits). The scattered vector $\mathbf{k}_{\rm out}$ is defined by the position of the detector at the angles β_i and β_o; the plane defined by $\mathbf{k}_{\rm in}$ and $\mathbf{k}_{\rm out}$ is called the scattering plane. The detector entrance is defined by two orthogonal sets of slits S_{D_i} and S_{D_o} perpendicular to $\mathbf{k}_{\rm out}$. The experimental resolution includes the wavelength dispersion, the beam angular divergence and the detector acceptance angles. In other words, $\mathbf{k}_{\rm in}$ and $\mathbf{k}_{\rm out}$ are not ideally defined, but dispersed. The dispersion relative to $\mathbf{k}_{\rm in}$ depends on the optical setup before the sample (source, monochromator *etc.*). The dispersion relative to $\mathbf{k}_{\rm out}$ comes from purely geometrical considerations. It is due to the existence of acceptance angles as defined by the detector slits and the illuminated area on the sample (footprint). The measured scattered intensity I results from averaging over the angular deviations and can be expressed as a function the wavevector transfer $\mathbf{q} = \mathbf{k}_{\rm out} - \mathbf{k}_{\rm in}$. It can be written as the convolution of the scattering function $S(\mathbf{q})$ with a resolution function $\mathcal{R}$ describing the distribution of the deviations $\mathbf{q}'$ around $\mathbf{q}$:

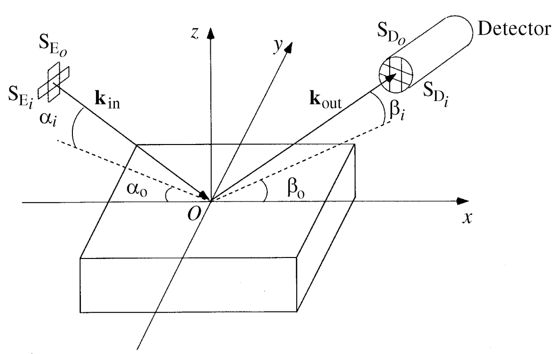

Figure 1
General scattering geometry of a z-axis (vertical) setup. The incidence plane is defined by the incident wavevector $\mathbf{k}_{\rm in}$ and the surface normal (Oz); the scattering plane is defined by the scattered wavevector $\mathbf{k}_{\rm out}$ and $\mathbf{k}_{\rm in}$.

$$I(\mathbf{q}) = \int S(\mathbf{q} - \mathbf{q}')\mathcal{R}(\mathbf{q}')\,{\rm d}\mathbf{q}'. \tag{1}$$

This formalism is appealing because it allows the advantageous use of the reciprocal-space representation of the scattering function $S(\mathbf{q})$. For instance, in the first Born approximation, S is simply given by the Fourier transform of the density–density correlation function:

$$S(\mathbf{q}) = \int {\rm d}^3 r \exp(\imath \mathbf{q} \cdot r)\langle \rho(0)\rho(\mathbf{r})\rangle. \tag{2}$$

Note that equation (1) is valid only in the incoherent limit. The effects of partial coherence have their importance especially when using synchrotron radiation and have been discussed elsewhere (Sinha *et al.*, 1998; Bernhoeft *et al.*, 1998).

So far, calculations of $\mathcal{R}$ have been limited to specific situations, such as specular reflectivity (Gibaud *et al.*, 1993), detector scans in the plane of incidence (de Jeu *et al.*, 1996) and Bragg diffraction (Holý *et al.*, 1999). In these geometries the incident and the scattering plane coincide and equation (1) boils down to simply averaging the scattering function over a resolution area in the plane of incidence. More complicated scattering geometries associated with surface diffraction (Vlieg, 1997) or scattering out of the plane of incidence (Mol *et al.*, 1997) require averaging over a full resolution volume. In such situations, $\mathcal{R}$ has not always been clearly analyzed. The aim of this paper is to present a general method to calculate $\mathcal{R}$. In §2, we derive a general form for the resolution function, taking into account the deviations associated with the beam dispersion and the detector acceptance angles. In §3, useful expressions relating reciprocal- and direct-space mean square deviations are derived for some common scattering geometries. In §4, a suitable method is given to determine the mean square values of the experimental parameters. Finally, in §5, we discuss the effect of the resolution on the particular example of scattering from free-standing smectic films.

2. General resolution function

Let us start with the description of dispersions relative to $\mathbf{k}_{\rm in}$ and $\mathbf{k}_{\rm out}$ by introducing random deviations $\alpha'_{i,o}$ and $\beta'_{i,o}$ around the angles $\alpha_{i,o}$ and $\beta_{i,o}$, respectively. In what follows we assume that $\alpha'_{i,o}$ and $\beta'_{i,o}$ can be described by a Gaussian distribution and are statistically independent. In this case they are fully described by their mean square deviations $\Delta\alpha^2_{i,o} = \langle(\alpha'_{i,o})^2\rangle$ and $\Delta\beta^2_{i,o} = \langle(\beta'_{i,o})^2\rangle$. Furthermore, we assume the random deviations to be small. This allows use of a linear relation between the angular deviations and $\mathbf{q}'$. From Fig. 1, the relation between $\mathbf{q}$ and the four angles is

$$\begin{cases} q_x = k(\cos\beta_i\,\cos\beta_o - \cos\alpha_i\,\cos\alpha_o), \\ q_y = k(\cos\beta_i\,\sin\beta_o + \cos\alpha_i\,\sin\alpha_o), \\ q_z = k(\sin\alpha_i + \sin\beta_i), \end{cases} \quad (3)$$

where $k = 2\pi/\lambda$, and λ is the wavelength. For the sake of simplicity, we assume the beam to be ideally monochromated, so that we can disregard the wavelength dispersion $\Delta\lambda$. After taking the partial derivatives, we obtain

$$\begin{cases} q'_x = k(\alpha'_i\,\sin\alpha_i\,\cos\alpha_o + \alpha'_o\,\cos\alpha_i\,\sin\alpha_o \\ \qquad - \beta'_i\,\sin\beta_i\,\cos\beta_o - \beta'_o\,\cos\beta_i\,\sin\beta_o), \\ q'_y = k(-\beta'_i\,\sin\beta_i\,\sin\beta_o + \beta'_o\,\cos\beta_i\,\cos\beta_o \\ \qquad - \alpha'_i\,\sin\alpha_i\,\sin\alpha_o + \alpha'_o\,\cos\alpha_i\,\cos\alpha_o), \\ q'_z = k(\alpha'_i\cos\alpha_i + \beta'_i\cos\beta_i). \end{cases} \quad (4)$$

These linear relations together with mean square deviations $\Delta\alpha^2_{i,o}$ and $\Delta\beta^2_{i,o}$ allow us to write down the mean square deviations of $\mathbf{q}$:

$$\begin{aligned} \langle q'_x q'_x\rangle &= k^2(\sin^2\alpha_i\,\cos^2\alpha_o\Delta\alpha_i^2 + \cos^2\alpha_i\,\sin^2\alpha_o\Delta\alpha_o^2 \\ &\quad + \sin^2\beta_i\,\cos^2\beta_o\Delta\beta_i^2 + \cos^2\beta_i\,\sin^2\beta_o\Delta\beta_o^2), \\ \langle q'_y q'_y\rangle &= k^2(\sin^2\alpha_i\,\sin^2\alpha_o\Delta\alpha_i^2 + \cos^2\alpha_i\,\cos^2\alpha_o\Delta\alpha_o^2 \\ &\quad + \sin^2\beta_i\,\sin^2\beta_o\Delta\beta_i^2 + \cos^2\beta_i\,\cos^2\beta_o\Delta\beta_o^2), \\ \langle q'_z q'_z\rangle &= k^2(\cos^2\alpha_i\Delta\alpha_i^2 + \cos^2\beta_i\Delta\beta_i^2), \\ \langle q'_x q'_y\rangle &= k^2(-\sin^2\alpha_i\,\sin\alpha_o\,\cos\alpha_o\Delta\alpha_i^2 \\ &\quad + \cos^2\alpha_i\,\sin\alpha_o\,\cos\alpha_o\Delta\alpha_o^2 \\ &\quad + \sin^2\beta_i\,\sin\beta_o\,\cos\beta_o\Delta\beta_i^2 \\ &\quad - \cos^2\beta_i\,\sin\beta_o\,\cos\beta_o\Delta\beta_o^2), \\ \langle q'_x q'_z\rangle &= k^2(-\sin\beta_i\,\cos\beta_i\,\cos\beta_o\Delta\beta_i^2 \\ &\quad + \sin\alpha_i\,\cos\alpha_i\,\cos\alpha_o\Delta\alpha_i^2), \\ \langle q'_y q'_z\rangle &= k^2(-\sin\alpha_i\,\sin\alpha_o\,\cos\alpha_i\Delta\alpha_i^2 \\ &\quad - \sin\beta_i\,\sin\beta_o\,\cos\beta_i\Delta\beta_i^2). \end{aligned} \quad (5)$$

The general resolution function $\mathcal{R}$, defined as the Gaussian joint-distribution function of the random deviations q'_x, q'_y, q'_z, is expressed as follows (*e.g.* van Kampen, 1981):

$$\mathcal{R}(\mathbf{q}') = [\det A^{-1}/(2\pi)^3]^{1/2}\exp[-(1/2)\mathbf{q}'\cdot A^{-1}\mathbf{q}'], \quad (6)$$

where $A = \langle q'_i q'_j\rangle$ is the covariance matrix of the random deviation $\mathbf{q}'$ as given by equation (5). The prefactor in equation (6) is simply a normalization factor. From here on, we assign the eigenvalues of A to be Δq_x^2, Δq_y^2 and Δq_z^2, and let (O, x, y, z) refer implicitly to the eigenvector coordinate system of A. Then the analytical convolution in equation (1) in combination with equation (2) leads to the following general expression for the intensity:

$$\begin{aligned} I = \textstyle\int \mathrm{d}^3 r\exp[\imath\mathbf{q}\cdot r - (1/2)x^2\Delta q_x^2 - (1/2)y^2\Delta q_y^2 \\ - (1/2)z^2\Delta q_z^2]\langle\rho(0)\rho(r)\rangle. \end{aligned} \quad (7)$$

The next step consists of carrying out the integration in equation (7). We will describe how to perform this integration in the case of diffuse scattering from free-standing smectic films in §5. The relation between the reciprocal- and direct-space mean square deviations is not straightforward. In the next section, we shall give some useful approximations for some common scattering geometries, such as rocking scans and diffuse scans out of the plane of incidence.

3. Application to specific scattering geometries

Let us consider first scattering geometries where $\mathbf{q}$ stays in the plane of incidence ($q_y = 0, \alpha_o = \beta_o = 0$). This is, for example, the case for so-called rocking scans (see Fig. 2) where $\omega = (\alpha_i - \beta_i)/2$ is varied, while $\theta = (\alpha_i + \beta_i)/2$ is kept constant. In this case q_x is varied while q_z is kept effectively almost constant over the accessible range determined by the constraint $|\omega| \leq \theta$. It also applies to detector scans in the plane of incidence, for which β_i is varied while α_i is kept constant (Daillant *et al.*,

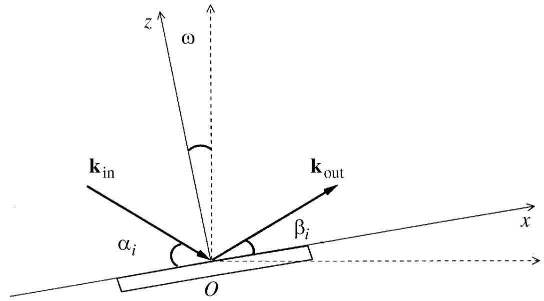

Figure 2
Scattering configuration of a rocking scan in which the angle $\omega = (\alpha_i - \beta_i)/2$ is varied in the xz plane of incidence ($q_y = 0$). In reciprocal space, q_x is varied over a range limited by the geometrical constraint $|\omega| \leq (\alpha_i + \beta_i)/2$, while q_z is kept practically constant.

1996). From equation (5), and keeping only leading order terms, A reads:

$$A/k^2 = \begin{Bmatrix} \alpha_i^2\Delta\alpha_i^2 + \beta_i^2\Delta\beta_i^2 & 0 & \alpha_i\Delta\alpha_i^2 - \beta_i\Delta\beta_i^2 \\ 0 & \Delta\alpha_o^2 + \Delta\beta_o^2 & 0 \\ \alpha_i\Delta\alpha_i^2 - \beta_i\Delta\beta_i^2 & 0 & \Delta\alpha_i^2 + \Delta\beta_i^2 \end{Bmatrix}. \tag{8}$$

It is clear from the covariance matrix that the eigenvalues Δq_x^2 and Δq_z^2 are strongly correlated, while Δq_y^2 is independent. This has important consequences for the resolution and the calculation of the intensity, as we will see below and in §5. In the limit of grazing angles in the plane of incidence (α_i, $\beta_i \lesssim 10^\circ$), we obtain the following leading order expressions for the reciprocal-space mean square deviations:

$$\begin{cases} \Delta q_x^2 \simeq k^2[\Delta\alpha_i^2\Delta\beta_i^2(\alpha_i+\beta_i)^2/(\Delta\alpha_i^2+\Delta\beta_i^2) \\ \qquad + (\alpha_i^2\Delta\alpha_i^2 + \beta_i^2\Delta\beta_i^2)^2/4], \\ \Delta q_y^2 \simeq k^2(\Delta\alpha_o^2 + \Delta\beta_o^2), \\ \Delta q_z^2 \simeq k^2(\Delta\alpha_i^2 + \Delta\beta_i^2). \end{cases} \tag{9}$$

Note that for $\alpha_i = \beta_i$ and $\Delta\alpha_i = \Delta\beta_i$, we obtain the first-order relation $\Delta q_x^2 = \alpha_i^2\Delta q_z^2$ previously derived by de Jeu *et al.* (1996). The condition $\Delta\alpha_i^2 \to 0$ depends on the beam characteristics and can be realised using synchrotron radiation or variable grating parabolic multilayer optics which produce highly parallel beams. During a diffuse scan, the eigenvector coordinate system rotates in the plane of incidence. In fact, for the case of rocking scans, the eigenvector coordinate system corresponds approximately to the original one because of the geometrical constraint $|\omega| \leq \theta$. Consequently, we can further simplify the calculation of the intensity in equation (7). One can open the detector slit S_{D_o} widely without modifying the relevant inplane resolution Δq_x^2 (see §5). In this way, Δq_y is sufficiently large to induce a fast decay of $\exp(-y^2\Delta q_y^2/2)$. Therefore, only the region $y \simeq 0$ will contribute to the integral, like in the case of a δ function. This allows us to keep in the integrand only $\langle\rho(0)\,\rho(x, y = 0, z)\rangle$ and reduces the calculation to a double integration over x and z only. In the reciprocal-space representation the resolution function is reduced to a function of q_x and q_z only. Information about q_y is lost as a result of the large smearing in the y direction, but does not influence the information about q_x. One finally arrives at an expression similar to equation (1):

$$I(q_x, q_z) = \int \mathrm{d}q_x'\,\mathrm{d}q_z'\,\mathbb{R}(q_x', q_z')\,S(q_x - q_x', q_z - q_z'), \tag{10}$$

but with $\mathbb{R}$ and S defined as

$$\mathbb{R}(q_x, q_z) = (1/2\pi\Delta q_x\Delta q_z)\exp[-(q_x^2/2\Delta q_x^2) - (q_z^2/2\Delta q_z^2)]$$

and

$$S(q_x, q_z) = [(2\pi)^{1/2}/\Delta q_y]\int \mathrm{d}x\mathrm{d}z\ \exp(\imath q_x x + \imath q_z z) \\ \times \langle\rho(0)\rho(x, y = 0, z)\rangle.$$

Now, let us consider the case of detector scans out of the plane of incidence, which are extensively used in solid-state surface diffraction experiments (Vlieg, 1997), and in diffuse scattering experiments on liquid surfaces (Mol *et al.*, 1997; Daillant *et al.*, 1996). As shown in Fig. 3, in this situation the detector is moved by an angle β_o while $\alpha_o = 0$. To optimize the diffuse signal, $\alpha_i = \beta_i$ is often used in addition. In this way, q_y and q_x are probed over a large and small range, respectively, while q_z is kept constant on the specular ridge, as deduced from equation (3). In this geometry, the scattering cross section is limited by the resolution in all directions in space. From equation (5), and keeping only leading order terms, A reads:

$$A/k^2 = \begin{Bmatrix} \begin{matrix}[\alpha_i^2(\Delta\alpha_i^2 + \Delta\beta_i^2) \\ +\beta_o^2\Delta\beta_o^2]\end{matrix} & -\beta_o\Delta\beta_o^2 & \alpha_i(\Delta\alpha_i^2 - \Delta\beta_i^2) \\ -\beta_o\Delta\beta_o^2 & \Delta\alpha_o^2 + \Delta\beta_o^2 & -\alpha_i\beta_o\Delta\beta_i^2 \\ \alpha_i(\Delta\alpha_i^2 - \Delta\beta_i^2) & -\alpha_i\beta_o\Delta\beta_i^2 & \Delta\alpha_i^2 + \Delta\beta_i^2 \end{Bmatrix}. \tag{11}$$

In the limit of grazing angles in the plane of incidence (α_i, $\beta_i \lesssim 10^\circ$), the in-plane eigenvalues Δq_x^2 and Δq_y^2 are strongly correlated, while Δq_z^2 does not depend on the inplane resolution. This will lead to radically different consequences

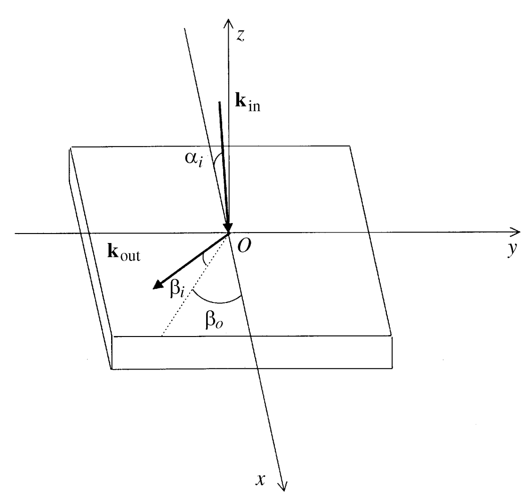

Figure 3
Scattering configuration of a scan out of the plane of incidence. The detector is moved over an angle β_o while α_o is constant (here taken as $\alpha_o = 0$). In the reciprocal space, q_x and q_y are probed over small and large ranges, respectively, while q_z is kept constant.

compared to diffuse scans in the plane of incidence, and will be illustrated in detail in §5. For grazing angles, we obtain the following useful approximations for the reciprocal-space mean square deviations:

$$\begin{cases} \Delta q_x^2 \simeq k^2[4\alpha_i^2 \Delta\alpha_i^2 \Delta\beta_i^2/(\Delta\alpha_i^2 + \Delta\beta_i^2) \\ \qquad + \beta_o^2 \Delta\alpha_o^2 \Delta\beta_o^2/(\beta_o^2 \Delta\beta_o^2 + \Delta\alpha_o^2 + \Delta\beta_o^2)], \\ \Delta q_y^2 \simeq k^2(\Delta\alpha_o^2 + \Delta\beta_o^2), \\ \Delta q_z^2 \simeq k^2(\Delta\alpha_i^2 + \Delta\beta_i^2). \end{cases} \tag{12}$$

Thus, the eigenvector coordinate system is essentially rotated in the plane of the sample. This property is particularly interesting for the study of liquid surfaces where the correlation function is isotropic in this plane. Note that in the limit $\beta_o \lesssim 10^\circ$, $\Delta q_x^2 \simeq k^2[4\alpha_i^2 \Delta\alpha_i^2 \Delta\beta_i^2/(\Delta\alpha_i^2 + \Delta\beta_i^2)]$, implying that $\Delta q_x^2 \ll \Delta q_y^2$. This large difference between Δq_x^2 and Δq_y^2 is interesting because the in-plane resolution $\Delta q_\parallel^2$, where the symbol $\|$ stands for the component in the plane of the sample (Oxy), determines the minimal accessible $q_\parallel$ range (see also §5). Hence, for liquid systems, the low-$q_\parallel$ range can be measured by q_x, while the high-$q_\parallel$ range is accessible by q_y, making it possible to record the fluctuation spectrum from macroscopic down to molecular dimensions.

4. Determination of the dispersion angles

The mean square deviations $\Delta\alpha_{i,o}^2$ account for the incident-beam angular dispersion, directly related to the beam divergence, which depends on the optical settings between the X-ray source and the sample. It contributes, together with the beam width due to the pre-sample entrance slits $S_{E_{i,o}}$, to the half width at half-maximum, $\mathrm{HWHM}_{i,o}$, of the intensity profile $I(\beta_{i,o})$ measured by a detector scan in or out of the plane of incidence. In such a scan, the angular distribution due to the beam width is a step function of width $\arctan(S_{E_{i,o}}/D)$, where D is the distance between the detector and the centre of the diffractometer (coinciding with O in Fig. 1). The measured intensity profile $I(\beta_{i,o})$ is convoluted with the detector slits $S_{E_{i,o}}$, and depends on D:

$$I(\beta_{i,o}) = I_0 \exp(-\beta_{i,o}^2 \ln 2/\mathrm{HWHM}_{i,o}^2) * \Pi(\beta_{i,o}), \tag{13}$$

with

$$\Pi(\beta_{i,o}) = \begin{cases} 1 & \text{if } |\beta_{i,o}| \le \arctan(S_{D_{i,o}}/D)/2, \\ 0 & \text{elsewhere.} \end{cases}$$

Assuming Gaussian distributions, we obtain the following relation for the angular mean square deviations of the incident beam:

$$\Delta\alpha_{i,o}^2 = \mathrm{HWHM}_{i,o}^2/(2\ln 2) - \arctan^2(S_{E_{i,o}}/D)/12. \tag{14}$$

The mean square deviations $\Delta\beta_{i,o}^2$ are related to the acceptance solid angle of the detector, which depends both on the illuminated area of the sample and on the detector slits, as shown in Fig. 4. The incident-beam divergence can be used to evaluate the effective footprint $L_{i,o}$ in and out of the plane of incidence, respectively. Two accepting angles, $\beta_{i,o}^{\min}$ and $\beta_{i,o}^{\max}$ define the angular distribution p of the intensity entering the detector aperture. Note that p also describes the intensity profile in the direction $\beta_{i,o}$, collected during a detector scan around $\beta_{i,o}$. An important consequence of this is discussed in §5. For $D \gg \max(L_{i,o}\sin\beta_{i,o}, S_{D_{i,o}})$, p has a trapezoidal form with top $2\beta_{i,o}^{\min}$ and base $2\beta_{i,o}^{\max}$. Explicitly, p reads

$$p(\beta'_{i,o}) = \begin{cases} 1/(\beta_{i,o}^{\max} + \beta_{i,o}^{\min}) & \text{if } |\beta'_{i,o}| < \beta_{i,o}^{\min} \\ \dfrac{(\beta_{i,o}^{\max} - \beta'_{i,o})}{[(\beta_{i,o}^{\max})^2 - (\beta_{i,o}^{\min})^2]} & \text{if } \beta_{i,o}^{\min} > \beta'_{i,o} > \beta_{i,o}^{\max} \\ 0 & \text{if } |\beta'_{i,o}| > \beta_{i,o}^{\max} \end{cases} \tag{15}$$

We replace this trapezoidal distribution by a Gaussian distribution giving the same mean square values, which leads to

$$\Delta\beta_{i,o}^2 = (1/6)[(\beta_{i,o}^{\min})^2 + (\beta_{i,o}^{\max})^2], \tag{16}$$

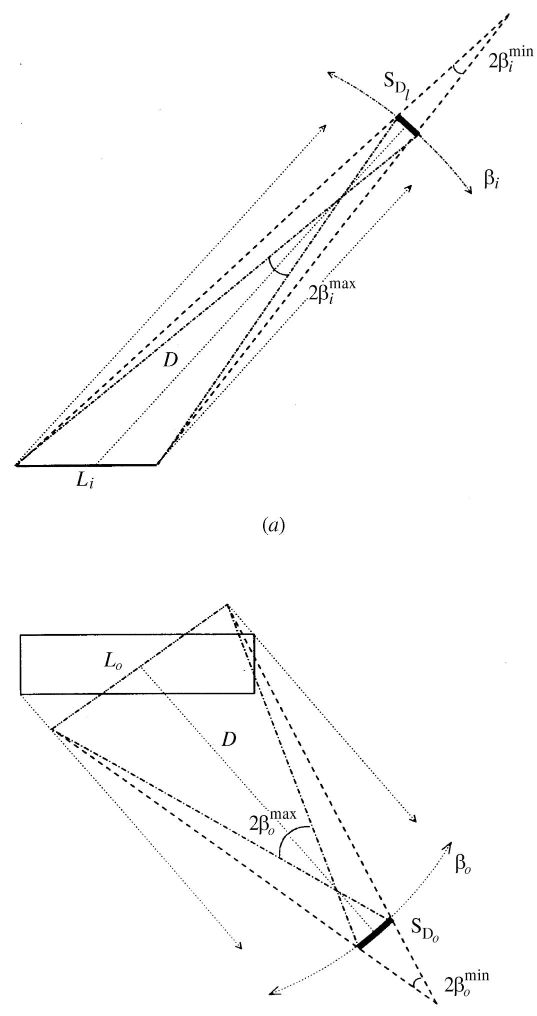

(a)

(b)

Figure 4
Acceptance angles $2\beta_{i,o}^{\min}$ and $2\beta_{i,o}^{\max}$ of the detector entrance defined by the detector slits $S_{D_{i,o}}$, the footprint $L_{i,o}$ on the sample and the distance D from the detector to the centre of the diffractometer. They describe the distribution of the specularly reflected intensity viewed by the detector during scanning as well as the intensity angular distribution viewed by the detector for a fixed position. (a) In the plane of incidence. (b) Out of the plane of incidence.

with $\beta_{i,o}^{\max}$ and $\beta_{i,o}^{\min}$ given by

$$\begin{aligned}\beta_{i,o}^{\max} - \beta_{i,o}^{\min} &\simeq [\max(L_{i,o}\sin\beta_{i,o}, S_{D_{i,o}})/D],\\ \beta_{i,o}^{\min} &\simeq |L_{i,o}\sin\beta_{i,o} - S_{D_{i,o}}|/2D.\end{aligned} \quad (17)$$

Note that at large $\beta_{i,o}$ the possible presence of guard slits, positioned just after the sample to limit the background noise, may lead to a cutoff in the detector acceptance angles (Fradin *et al.*, 1998).

5. X-ray scattering from free-standing smectic films

In the case of a free-standing smectic A film, the scattering function is of the form (Shalaginov & Romanov, 1993; Mol *et al.*, 1996)

$$S(\mathbf{q}) = R_F \int \mathrm{d}\mathbf{r}_\parallel \exp(\imath \mathbf{q}_\parallel \cdot \mathbf{r}_\parallel)\, G(q_z, r_\parallel), \quad (18)$$

where $R_F \propto 1/q_z^4$ is the Fresnel reflectivity and $G(q_z, r_\parallel)$ is the height–height correlation function given by

$$\begin{aligned}G(q_z, r_\parallel) &= d\sum_{m,n}^{N} \exp[\imath q_z(m-n)d - (1/2)q_z^2 g_{mn}(r_\parallel)],\\ g_{mn}(r_\parallel) &= \langle [u_m(0) - u_n(r_\parallel)]^2\rangle.\end{aligned} \quad (19)$$

In equation (19), d is the smectic layer spacing, and $u_n(r_\parallel)$ is the displacement of the layer n along the (Oz) direction. It has been shown that in general thin smectic A films fluctuate conformally, which means that $g_{mn}(\mathbf{r}_\parallel)$ does not depend on n, m:

$$g(r_\parallel) = (k_BT/2\pi\gamma)[\ln(r_\parallel/r_0) + K_0(r_\parallel/r_0) + c - \ln 2], \quad (20)$$

where K_0 is the modified Bessel function, $c \simeq 0.5772$ is Euler's constant, $r_0 = (LK/2\gamma)^{1/2}$, with γ representing the surface tension, K the layer bending elasticity modulus, and $L = Nd$ the thickness of the film. In the case of scattering out of the plane of incidence, it is convenient to introduce in equation (11) the further simplification $Axz = Ayz = 0$. As a consequence, the convolution in the xy plane and the z direction can be carried out independently. This approximation has consequences for the value of Δq_x^2 but has no disturbing effects in q_y scans. A major problem comes from the fact that G decays roughly as $r_\parallel^{-\eta}$, where the exponent $\eta = q_z^2 k_B T/(4\pi\gamma)$ can be estimated to be given by $\eta \simeq 0.04$, taking $\gamma \simeq 20$ mN m^{-1}, $q_z \simeq 0.2$ Å^{-1} and $k_{BT} \simeq 4.5 \times 10^{-21}$ J. As a result, G decays very slowly, which may cause numerical problems when evaluating equation (7). To appreciate the problem one can take $G = 1$ and carry out the integration in equation (1) over the xy plane analytically, which yields a coefficient $\exp(-q_x^2/2\Delta q_x^2 - q_y^2/2\Delta q_y^2)$. If we take typical parameters at high q_y, namely $q_x \simeq 10^{-3}$ Å^{-1}, $q_y \simeq 0.1$ Å^{-1}, $\Delta q_x \simeq 10^{-5}$ Å^{-1}, $\Delta q_y \simeq 10^{-3}$ Å^{-1}, this coefficient becomes extremely small, $\sim\exp(-5000)$. Calculating numerically such a small value by a two-dimensional integration of oscillating functions requires long times and high precision. To facilitate the numerical calculation, we can use another representation, which turns out to be more efficient. We take advantage of the symmetry of the system and perform the integration over the xy plane in the following way:

$$\begin{aligned}&\textstyle\iint \mathrm{d}x\mathrm{d}y \exp[i(q_x x + q_y y) - (1/2)x^2\Delta q_x^2 - (1/2)y^2\Delta q_y^2] G(q_z, r_\parallel)\\ &\quad = (1/\Delta q_x \Delta q_y) \textstyle\int \mathrm{d}^2 q' \mathrm{d}r_\parallel r_\parallel J_0(|\mathbf{q} - \mathbf{q}'| r_\parallel)\\ &\qquad \times \exp[-q_x'^2/2\Delta q_x^2 - q_y'^2/2\Delta q_y^2] G(q_z, r_\parallel),\end{aligned} \quad (21)$$

where J_0 is the Bessel function of order zero. Although this procedure requires an additional integration, it is much more efficient because the range of integration is smaller than in equation (7).

In the case of systems with a finite correlation distance, $G(q_z, r_\parallel)$ would decay exponentially to a constant value $G(q_z, \infty) \simeq \exp[-q_z^2\langle u(0)^2\rangle]$. Integration of this constant with $\exp(\imath \mathbf{r}_\parallel \cdot \mathbf{q}_\parallel)$ provides a δ function. In such a situation there are good reasons to split the total intensity into two parts. The first one is the specular reflectivity due to $G(q_z, \infty)$; the second is the diffuse scattering due to $[G(q_z, r_\parallel) - G(q_z, \infty)]$ in the integrand. The specular reflectivity can be analysed separately using, for example, the matrix formalism of Parrat (1954). To carry out this type of analysis one has to subtract the diffuse contribution to the specular signal which arises because of the finite size of the detector aperture. This requires the resolution treatment to be modified accordingly (Shindler & Suter, 1992). In the case of smectic liquid crystals, the situation is different because the mean square displacement fluctuations diverge due to Landau–Peierls instability (*e.g.* de Gennes & Prost, 1993; Vertogen & de Jeu, 1988). Therefore, no correlation distance can be identified to which the height–height correlation function $G(q_z, r_\parallel)$ decays: the function $\langle [u_m(0) - u_n(r_\parallel)]^2\rangle$ tends formally to infinity as $r_\parallel$ increases. As a result, G decays algebraically to zero and we face the following features. In the first place, there is no basis to split the intensity into two parts. Secondly, the integral in equation (18) diverges and only the convolution with the resolution function makes it finite. Consequently, the accessible range for the fluctuation spectrum depends on the parametrization of the resolution function.

Let us now analyse the combined effect of the resolution and correlation functions on the scattered intensity in the cases of diffuse scans in and out of the plane of incidence, where $I(q_\parallel)$ is probed as described in §3. The major effect of the resolution is to limit the flux of scattered intensity in the detector and to broaden the structural details in $I(q_\parallel)$. In the case of thin films, the main signature of structural details comes from the Fresnel factor $R_F(q_z)$ in equation (18) and results in interference fringes, called Kiessig fringes (Born & Wolf, 1980). For a detector scan in the plane of incidence, q_z is varied and the Kiessig fringes are smeared out by the resolution. For diffuse scans out of the plane of incidence, q_z is kept constant and the resolution has no smearing effects. Another important feature is related to the distinction between specular and off-specular dominated regions. One may define a specular region $I_{\rm spec}(q_z) = I(q_\parallel \simeq 0)$ corresponding to a certain positional range of the detector in the domain of the specularly reflected beam sheet. As already mentioned in §4, $\Delta q_\parallel^2$ corresponds to the mean square deviation of the intensity distribution $I(q_{\|})$ collected by a detector scan around $q_{\|}$ (see Fig. 4). Therefore, the region corresponding to $0 \lesssim q_{\|} \lesssim \Delta q_{\|}$ is dominated by the specularly reflected intensity. In particular, this may provide a method to subtract the pure diffuse scattering from the totally reflected intensity. The diffuse region is influenced both by the resolution and the correlation function. More precisely, the correlation function influences the slope of the diffuse scattering in different manners depending on the type of resolution and geometry used. As a result, beyond the 'plateau region', the in-plane resolution factor in equation (21) has no effect on the shape of the scattering. Thus, there exists an intermediate $q_{\|}$ region where the logarithmic term in $g(r_{\|})$ is dominant (in between the 'plateau' and high $q_{\|}$ regions). In this region, the intensity follows an algebraic decay law of the following type:

$$I(q_{\|}) \simeq \int \mathrm{d}\mathbf{r}_{\|} \exp(\imath \mathbf{q}_{\|} \cdot \mathbf{r}_{\|}) r_{\|}^{-\eta} \simeq q_{\|}^{-D+\eta}, \qquad (22)$$

where $D = 1$ or 2, depending on whether a one- or two-dimensional integration is performed. At higher $q_{\|}$ regions, we expect a nonlinear deviation from the algebraic decay to be induced by the bending elasticity modulus K.

Let us now check the points raised in the above discussion using some concrete examples. Fig. 5 shows calculations of the scattering in or out of the plane of incidence from a smectic film computed with the same physical parameters (γ, K, d, N) used in $G(q_z, r_{\|})$ above. The left curves are rocking scans using one- or two-dimensional integration [performed with or without detector slit S_{D_o}, respectively] and using the covariance matrix (8). The right curve is a detector scan out of the plane of incidence using necessarily a two-dimensional integration and the covariance matrix (11). All the curves exhibit a large 'plateau' region at low $q_{\|}$ distinct from a smooth negative slope starting at $q_{\|} \simeq \Delta q_{\|}$. As explained above, the first part can be associated with the specularly reflected intensity and the second part with the off-specular intensity. The slope behaviour of the diffuse part is clearly dominated by the correlation function. Indeed, there are large intermediate regions having slopes either close to $q_{\|}^{-1+\eta}$ for a rocking scan without detector slit S_{D_o} (left solid line), or close to $q_{\|}^{-2+\eta}$ for a diffuse scan out of the plane of incidence (right solid line) as a result of the dimensionality of the integration in equation (22). The effect of the bending elasticity modulus K occurs at higher $q_{\|}$ and results in a strong nonlinear attenuation of the diffuse intensity, as can be seen in detector scans out of the plane of incidence (right solid line). Note that for rocking scans it is difficult to reach sufficiently high values of $q_{\|}$ to see this effect because of the geometrical constraints (see Fig. 2).

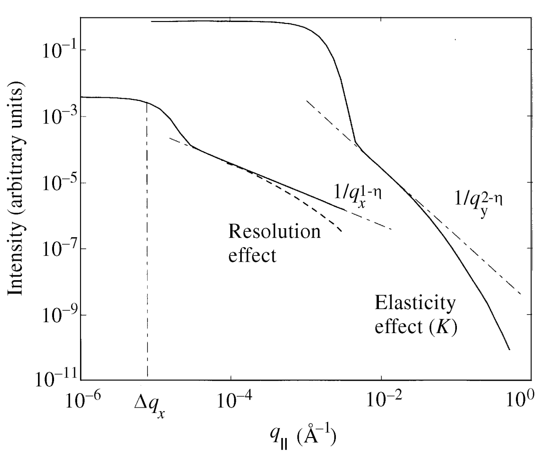

Figure 5
Calculation of the scattering from free-standing smectic films as explained in the text. Both curves exhibit two distinct parts: a 'plateau' region corresponding to the specular part, and a region exhibiting a smooth negative slope corresponding to the diffuse part. The fall-off of the 'plateau' corresponds to $q_{\|} \simeq \Delta q_{\|}$. Right solid line: diffuse scan out of the plane of incidence using a two-dimensional integration (slope $1/q^{2-\eta}$). Left solid line: rocking scan without detector slit S_{D_o} using a one-dimensional integration (slope $1/q^{1-\eta}$). Left dashed line: same rocking scan with a detector slit S_{D_o} of finite size added leading to an intermediate slope regime between $1/q^{2-\eta}$ and $1/q^{1-\eta}$.

Finally, we note that the interplay between resolution and correlation functions can change in a subtle way depending on the geometry of the experiment. This is illustrated Fig. 5 for the rocking scan upon introducing a finite vertical detector slit S_{D_o} (see left dashed line). In this case, a two-dimensional integration is performed as in equation (21). However, because $q_y = 0$ for a rocking scan, a slope regime between $q_{\|}^{-1+\eta}$ and $q_{\|}^{-2+\eta}$ is obtained. Note that the shape of the 'plateau' region remains unchanged upon addition of S_{D_o} because the relevant in-plane resolution component Δq_x^2 does not depend on Δq_y^2.

When one wishes to extract information from the off-specular scattering, it can be useful to adjust the resolution in order to obtain a minimal size of the 'plateau' region and a maximal flux of diffuse intensity in the detector. The first condition is fulfilled by minimizing the value of $\Delta q_{\|}^2$, which means using a rather parallel beam with relatively narrow detector slits in the direction of scanning. Furthermore, specific conditions depend on the geometry of the experiment, in particular on the type of correlations between the resolution components Δq_x^2, Δq_y^2 and Δq_z^2, as already discussed in section §3. In the case of diffuse scans in the plane of incidence, the relevant in-plane resolution Δq_x^2 does not change when Δq_y^2 is varied. Therefore, it is a good strategy to open the vertical detector slit S_{D_o} widely to increase the flux of intensity in the detector without loosing the relevant in-plane resolution Δq_x^2. In the case of diffuse scans out of the plane of incidence, Δq_x^2 and Δq_y^2 are correlated. However, in this geometry, the vertical resolution Δq_z^2 does not depend on the in-plane resolution. Therefore, it is an interesting strategy to open the horizontal slit S_{D_i} widely to increase the flux in the detector without loosing the resolution Δq_y^2 corresponding to the high-$q_{\|}$ range probed.

6. Conclusion

We have given a comprehensive description of the resolution function in the context of grazing-angle X-ray scattering experiments. We have shown how to calculate the resolution function $\mathcal{R}$ and have given explicit expressions relating the mean square deviations of $\mathbf{q}'$ and of the relevant direct-space angles for some common scattering configurations. For these scattering geometries, we have used the formalism given to calculate the scattering from free-standing smectic films in order to analyse the shape of the scattered intensity $I(\mathbf{q}_{\|})$. In particular, we have defined two regions, a 'plateau' region for $\mathbf{q}_{\|} \lesssim \Delta\mathbf{q}_{\|}$, which can be associated with the specularly reflected intensity, and a purely diffuse region for $\mathbf{q}_{\|} \gtrsim \Delta\mathbf{q}_{\|}$, in which we have described the combined influence of the correlation and the resolution functions for each scanning geometry.

We would like to thank J. Daillant and D. S. Dean for useful discussions. This work is part of the research programme of the 'Stichting voor Fundamenteel Onderzoek der Materie' (Foundation for the Fundamental Research of Matter, FOM) which is financially supported by the 'Nederlandse Organisatie voor Wetenschappelijk Onderzoek' (Netherlands Organization for the Advancement of Research, NWO). DS acknowledges support from the TMR Programme of the European Union (contract ERBFMICT 9828877). ANS acknowledges hospitality during multiple visits to Amsterdam.

References

Bernhoeft, N., Hiess, A., Langridge, S., Stunault, A., Wermeille, D., Vettier, C., Lander, G. H., Huth, M., Jourdan, M. & Adrian, H. (1998). *Phys. Rev. Lett*. **81**, 3419–3422.

Born, M. & Wolf, E. (1980). *Principles of Optics*. London: Pergamon.

Daillant, J., Quinn, K., Gourier, C. & Rieutord, F. (1996). *J. Chem. Soc. Faraday Trans.* **92**, 505–513.

Fradin, C., Braslau, A., Luzet, D., Alba, M., Gourier, C., Daillant, J., Grübel, G., Vignaud, G., Legrand, J. F., Lal, J., Petit, J. M. & Rieutord, F. (1998). *Physica B*, **248**, 310–315.

Gennes, P. G. de & Prost, J. (1993). *Physics of Liquid Crystals*. Oxford: Clarendon.

Gibaud, A., Vignaud, G. & Sinha, S. K. (1993). *Acta Cryst.* A**49**, 642–648.

Gompper, G. & Schick, M. (1994). *Self-Assembling Amphiphilic Systems*, *Phase Transitions and Critical Phenomena*. London: Academic.

Holý, V., Pietsch, U. & Baumbach, T. (1999). *High-Resolution X-ray Scattering from Thin Films and Multilayers*. Berlin: Springer.

Jeu, W. H. de, Shindler, J. D. & Mol, E. A. L. (1996). *J. Appl. Cryst.* **29**, 511–515.

Kampen, N. G. van (1981). *Stochastic Processes in Physics and Chemistry.* Amsterdam: North-Holland.

Mol, E. A. L., Shindler, J. D., Shalaginov, A. N. & de Jeu, W. H. (1996). *Phys. Rev. E*, **54**, 536–549.

Mol, E. A. L., Wong, G. C. L., Petit, J. M., Rieutord, F. & de Jeu, W. H. (1997). *Phys. Rev. Lett.* **79**, 3439–3442.

Parrat, L. G. (1954). *Phys. Rev.* **95**, 359–369.

Shalaginov, A. N. & Romanov, V. P. (1993). *Phys. Rev. B*, **48**, 1073–1083.

Shindler, J. D. & Suter, R. M. (1992). *Rev. Sci. Instrum.* **63**, 5343–5347.

Sinha, S. K., Tolan, M. & Gibaud, A. (1998). *Phys. Rev. B*, **57**, 2740–2758.

Tolan, M. (1999). *X-ray Scattering from Soft-Matter Thin Films*, *Material Science and Basic Research.* Berlin: Springer.

Vertogen, G. & & de Jeu, W. H. (1988). *Thermotropic Liquid Crystals*, *Fundamentals*. Berlin: Springer.

Vlieg, E. (1997). *J. Appl. Cryst.* **30**, 532–543.